LAWRENCE
LIVERMORE
NATIONAL
LABORATORY

LLNL-JRNL-724260

Enhancement of antigen-specific CD4+ and CD8+ T cell responses using a self-assembled biologic nanolipoprotein particle vaccine.

D. Weilhammer, A. Dunkle, C. Blanchette, N. Fischer, M. Corzett, D. Lehmann, T. Boone, P. Hoeprich, A. Driks, A. Rasley

February 16, 2017

Vaccine

Disclaimer

Enhancement of antigen-specific CD4+ and CD8+ T cell responses using a self-assembled biologic nanolipoprotein particle vaccine

Dina Weilhammer[a,*], Alexis D. Dunkle[a,*,1], Craig D. Blanchette[a,2], Nicholas O. Fischer[a], Michele Corzett[a], Doerte Lehmann[b], Tyler Boone[b], Paul Hoeprich[a], Adam Driks[b] and Amy Rasley[a]

Affiliations:

[a]Biosciences and Biotechnology Division, Lawrence Livermore National Laboratory

[b]Department of Microbiology & Immunology, Loyola University Medical Center

Corresponding author:

Amy Rasley, Ph.D.

Rasley2@llnl.gov

Ph: 925-423-1284

Fax: 925-422-2282

[*] These authors contributed equally

[1] Present address:
Department of Biological Technologies, Genentech Inc, South San Francisco, CA

[2]Present address:
Department of Protein Chemistry/Structural Biology Department, Genentech Inc, South San Francisco, CA

ACKNOWLEDGEMENTS

Funding for this research was provided by the NIH/NIAID (R01AI093493-01 to A. Driks) and Laboratory Directed Research and Development (11-ERD-016 to A.R.). We would like to thank Cheri Lychak for her technical assistance on this project. This work was performed under the auspices of the U.S. Department of Energy by Lawrence Livermore National Security, LLC, Lawrence Livermore National Laboratory under Contract DE-AC52-07NA27344. LLNL-JRNL-724260.

CONFLICT OF INTEREST

The authors have no conflict of interest.

Abstract word count: 150

Manuscript word count: 2989

Number of references: 34

Number of figures: 4

ABSTRACT

To address the need for vaccine platforms that induce robust cell-mediated immunity, we investigated the potential of utilizing self-assembling biologic nanolipoprotein particles (NLPs) as an antigen and adjuvant delivery system to induce antigen-specific murine T cell responses. We utilized OT-I and OT-II TCR-transgenic mice to investigate the effects of NLP-mediated delivery of the model antigen ovalbumin (OVA) on T cell activation. Delivery of OVA with the TLR4 agonist monophosphoryl lipid A (MPLA) in the context of NLPs significantly enhanced the activation of both $CD4^+$ and $CD8^+$ T cells *in vitro* compared to co-administration of free OVA and MPLA. Upon intranasal immunization of mice harboring TCR-transgenic cells, NLPs enhanced the adjuvant effects of MPLA and the *in vivo* delivery of OVA, leading to significantly increased expansion of $CD4^+$ and $CD8^+$ T cells in lung-draining lymph nodes. Therefore, NLPs are a promising vaccine platform for inducing T cell responses following intranasal administration.

KEY WORDS

Nanolipoprotein, nanoparticle, intranasal, vaccine, T cell activation, nanodisc

INTRODUCTION

Current vaccine development efforts have shifted largely toward developing subunit vaccines capable of generating both cellular and humoral immunity [1]. While subunit vaccines benefit from improved safety profiles, they lack the immunogenicity of live attenuated or heat-killed vaccines and require the use of stimulatory adjuvants to elicit long-lasting immunity [2]. Furthermore, vaccines capable of inducing robust cell mediated immune responses are necessary to combat intracellular pathogens and tumors [1]. However, the use of alum as an adjuvant provokes a strong Th2 response resulting primarily in antibody generation, rather than a robust Th1 cytotoxic T cell response, to the antigen [3, 4]. Therefore, the development of vaccine formulations that integrate newly identified adjuvants and novel delivery platforms that can generate strong Th1 immune responses is paramount.

Nanoparticles have been widely explored as vaccine delivery platforms and offer a number of benefits including improved immunogenicity, reduced toxicities associated with high doses of adjuvants, improved pharmacokinetic profiles, and enhanced stability [2, 5, 6]. As soluble proteins are poorly internalized and have limited access to the cross-presentation pathway [9], strategies aimed at enhancing antigen uptake and processing by dendritic cells are critical for the development of subunit vaccines against intracellular pathogens and tumors. Nanoparticle-based vaccines that contain co-localized antigen and adjuvant provide two-fold benefits in this context. First, they present antigens in particulate form, which are internalized by dendritic cells more readily than soluble antigens [9]. Second, co-delivery of adjuvants serves to markedly enhance antigen processing, thus resulting in more efficient cross-presentation [10].

Despite a significant expansion in our understanding of innate and adaptive immunity, the development of vaccines comprised of new adjuvants and formulations remains largely unachieved [3, 4]. While Toll-like receptor (TLR) ligands, such as lipopolysaccharide (LPS), function as potent adjuvants and may induce more balanced T cell responses than alum, the non-specific toxicity and widespread inflammation associated with natural TLR ligands has limited their clinical translation to date. As such, approaches to mitigate these limitations are critical.

Nanolipoprotein particles (NLPs) are self-assembling, discoidal particles comprising a lipid bilayer stabilized by scaffold proteins, i.e. apolipoproteins. NLPs are well-tolerated both *in vitro* and *in vivo* and can be delivered by multiple routes with intranasal administration resulting in retention for at least 24 hours in the lungs [16]. Importantly, NLPs can be functionalized to incorporate TLR agonists which greatly enhances the activity and delivery of these compounds *in vitro* and *in vivo* [17]. Further, incorporation of both antigen and adjuvant onto NLPs significantly enhances antibody responses in mice compared with non-NLP conjugated control formulations [18].

To investigate the effects of NLPs on T cell responses, we utilized OT-I and OT-II transgenic mice, which have T cell receptors (TCRs) that are engineered to recognize peptides derived from the model antigen ovalbumin (OVA) displayed in the context of class I (OT-I) or class II (OT-II) MHC molecules. Since the specific TCRs expressed on OT-I and OT-II T cells are known, these cells can be easily identified by antibody staining, thus allowing the evaluation of $CD8^+$ and $CD4^+$ (respectively) T cell responses to OVA formulated with NLPs. The OVA and OT-I/OT-II model systems are well-characterized, robust models to assess T cell responses to vaccine formulations, including particle-based

vaccines [19-21]. We investigated the intranasal route of immunization to evaluate the potential for NLP-based vaccines against inhaled pathogens. Delivery of OVA on NLPs significantly enhanced the activation of T cells both *in vitro* and *in vivo* upon intranasal immunization. *In vitro*, this effect correlated with increased uptake of OVA by APCs, while *in vivo*, the data suggest that NLPs enhance both antigen delivery and the adjuvant effects of MPLA.

MATERIALS AND METHODS

Materials for NLP assembly

1,2-dioleoyl-*sn*-glycero-3-phosphocholine (DOPC) and synthetic MPLA (PHAD™) were purchased from Avanti Polar Lipids (Alabaster, AL). All other reagents were ordered from Sigma-Aldrich (St. Louis, MO). N-Hydroxysuccinimide -polyethyleneglycol 4-dibenzylcyclooctyne (NHS-PEG_4-DBCO) was purchased from Click Chemistry Tools (Scottsdale, AZ). The C18-PEG_6-N_3 molecule was custom synthesized by Creative PEGworks (Winston Salem, NC).

Preparation and characterization of adjuvanted NLPs and OVA conjugation

The NLP scaffold protein apoE422k (N-terminal 22 kDa fragment of apolipoprotein E4 (apoE4)) was expressed and purified using a similar protocol as previously described [26, 27]. MPLA was incorporated into the NLP using published procedures [18]. To covalently conjugate OVA to the MPLA-adjuvanted NLPs using click chemistry, an azide-bearing lipidic molecule (C18-PEG_6-N_3) was incorporated into the NLP bilayer during assembly to form MPLA:N_3NLPs, as previously described [16]. Incorporation of MPLA and the N_3-bearing molecule into MPLA:N_3NLPs was assessed by reverse phase HPLC as described previously [17]. For additional detailed information regarding MPLA:N_3NLP assembly and MPLA quantification, as well as OVA conjugation and subsequent fluorescent labeling, please see supplementary materials.

Mice

All animal work was conducted in accordance with protocols approved by the Lawrence Livermore National Laboratory Institutional Animal Care and Use Committee. OT-I and OT-II breeding pairs were obtained from The Jackson Laboratory (Sacramento, CA) and were maintained in PHS-assured facilities. OT-I transgenic animals were maintained as hemizygous by crossing to wild-type C57BL/6, while OT-II mice were homozygous. C57BL/6 mice were obtained from Harlan Laboratories (Livermore, CA).

Activation of OT-I and OT-II T cells and splenic APCs

Spleens from OT-I, OT-II or wild-type C57BL/6 mice were collected in cold PBS and made into a single-cell suspension by manual dissociation as described previously [17]. Cells were plated into 96-well plates at a density of 4 x 10^6 cells/ml in 200 μl per well in complete RPMI medium (10% FBS, 1x L-gluatamine, and 1x penicillin/streptomycin (all cell culture reagents from Gibco/Life Technologies, Grand Island, NY) containing 2 ng/ml IL-7 (PeproTech, Rocky Hill, NJ) to promote survival of all T cells. Final concentrations of OVA and MPLA were 3 μg/ml and 0.41 μg/ml, respectively. Cells were incubated at 37°C with 5% CO_2 for 4 or 24 hours, then stained for flow cytometric analysis.

OT-I/II cell transfer and intranasal immunizations

One day before immunization, spleens from OT-I or OT-II mice were collected in cold PBS and made into a single-cell suspension by manual dissociation, as described above. Cells were diluted to 10^7 cells/ml, and 100 μl (10^6 OT-I or OT-II splenocytes) were transferred to naïve C57BL/6 recipients via intraperitoneal injection. The next day, mice were lightly anesthetized using isoflurane, and OVA preparations (or PBS control) were administered

intranasally in 2 volumes of 15 μl each (one drop/nare; 30 μl/mouse). The doses administered per mouse ranged between 3-10 μg OVA and 0.41-0.5 μg MPLA (depending on the batch of particles used) or the equivalent conjugated to NLPs. Lymph nodes (LNs, mediastinal and inguinal) were collected seven days later and processed for staining. LNs were gently crushed into a single cell suspension in 2% FBS in PBS using a tissue homogenizer tube and pestle then lysed of RBCs, rinsed, and resuspended for staining (typically 0.5-1 x 10^6 cells per stain).

Flow cytometry

Lymph node cells or cultured splenocytes were resuspended in FACS Buffer (2% FBS in PBS with 0.1% NaN_3) containing 0.25-0.5 μl Mouse BD Fc Block (Clone 2.4G2, BD Pharmingen, San Diego, CA) and were kept on ice throughout staining. Surface-staining antibodies were added at dilutions of 1/200-1/2,000, and cells were incubated on ice for 20-30 min. Cells were washed and resuspended in 200 μl FACS Buffer for analysis on a FACSCaliber (BD Biosciences, San Jose, CA). Antibodies against cell-surface antigens were obtained from either BD Biosciences or Biolegend (San Diego, CA).

Analysis of OVA uptake

Splenocytes from wild-type C57BL/6 mice were processed and incubated with fluorescently-labeled OVA formulations as described for the activation of OT-I/II cells. After an incubation of 1 hour, cells were collected and surface stained as described above. Following surface staining, cells were incubated with anti-AF488 antibody from Life Technologies (Carlsbad, CA) at 1/100 for 30 min prior to analysis by flow cytometry. For

permeabilized cell experiments, cells were stained first for surface makers then fixed and permeabilized using the BD FACSPerm kit as indicated in the manufacturer's instructions. Cells were then incubated with anti-AF488 antibody in PermWash buffer for 30 min prior to analysis by flow cytometry. APCs were defined as B cells (CD19+), macrophages (CD11b+ CD11c-) or dendritic cells (CD11c+).

Data analysis and statistics

Data were analyzed and graphed using FlowJo (TreeStar, Ashland, OR) and Prism (GraphPad, La Jolla, CA) software. Differences between groups were analyzed for statistical significance using one-way ANOVA with Tukey's multiple comparisons test. An adjusted p value of 0.05 or less was considered significant, and significant differences are indicated as follows: *$p < 0.05$, **$p < 0.01$, ***$p < 0.001$, ****$p < 0.0001$.

RESULTS

Attachment of OVA to MPLA-containing NLPs (MPLA:NLPs)

Previously, we developed a novel method for conjugating recombinant protein antigens containing a poly-histidine (His) tag onto NLPs by utilizing nickel-chelating lipids [16, 18, 28, 29]. To incorporate OVA lacking a His tag, we utilized click chemistry to covalently attach OVA to lipids comprising the NLP bilayer [16]. Briefly, NLPs were prepared with 2 mol% C18-PEG6-N_3 and 2.5 mol% MPLA using the standard self-assembly reaction (referred to as MPLA:N_3NLPs) (Figure 1A). Free amines on OVA were labeled with NHS-DBCO to form OVA-DBCO as previously described [16]. The OVA-DBCO is reactive towards azide groups through a copper-free azide-alkyne cycloaddition reaction, forming a covalent bond. Conjugation of OVA-DBCO to MPLA:N_3NLPs was assessed by size-exclusion chromatography (SEC) analysis and SDS-PAGE analysis (Figure 1B, C). OVA-DBCO was incubated with the MPLA:N_3NLPs at different OVA-DBCO to MPLA:N_3NLPs molar ratios (0 – 160) overnight and then run on SEC. The resulting SEC chromatograms contained two peaks, where the first peak corresponded to retention times (t_R) consistent with OVA-DBCO:MPLA:N_3NLP (referred to as OVA:MPLA:N_3NLPs in the remaining text) and the second peak corresponded with the t_R of unreacted OVA-DBCO (Figure 1B). As expected there was an increase in the intensity and shift to larger sizes (decrease in t_R) as the OVA-DBCO to MPLA:N_3NLP ratio increased, which indicates successful attachment of OVA-DBCO [16].

To quantify the degree of conjugation and demonstrate that the increase in peak intensity and decrease in t_R were due to conjugation of the OVA-DBCO protein, the peak corresponding to the OVA:MPLA:N_3NLP constructs was analyzed by SDS-PAGE and

quantified by densitometry. As shown in Figure 1C (inset), both E422k and OVA-DBCO were present in the OVA:MPLA:N_3NLP SEC fractions, further demonstrating that the OVA-DBCO was successfully conjugated to the MPLA:N_3NLPs. When final conjugate ratios were expressed as a function of the initial reaction ratio (Figure 1C), a linear relationship was observed up to 100 proteins per MPLA:N_3NLP. Based on the slope of this linear relationship, the reaction was determined to be approximately 20% efficient. In the case of OVA, which is abundantly available, this inefficiency is not of particular concern, and free OVA was removed from OVA:MPLA:N_3NLP formulations for all studies.

Enhanced activation of OT-I and OT-II T cells by OVA:MPLA:NLPs

To determine the effect of delivery of OVA with or conjugated to MPLA:N_3NLPs on antigen presentation and T cell activation, we cultured total splenocytes from wild type (WT), OT-I, and OT-II mice with different OVA formulations or saline control. OVA (3 μg/ml) was administered alone, with free MPLA adjuvant, with MPLA:N_3NLPs (OVA not attached), and covalently bound to MPLA: N_3NLPs (OVA:MPLA: N_3NLP). Based on the relative incorporation of OVA and MPLA into the N_3NLPs in the fully conjugated formulation, a dose of 0.41 μg/ml MPLA was used for all formulations. A 10-fold lower dose of OVA/MPLA (0.3 μg/ml/0.041 μg/ml) was not as potent for activating T cells in a pilot experiment, likely due to the low a concentration of OVA, although similar trends to the higher dose experiments were observed (data not shown).

After 24 hours in culture with or without OVA, T cells ($CD3^+$) were analyzed for expression of the early activation markers CD25 and CD69 as well as upregulation of CD44 (Figure 2). We observed that a significantly larger percentage of T cells were activated

upon treatment with OVA:MPLA:N_3NLP compared to all other formulations. This result was observed in OT-I and OT-II spleens, but not WT, indicating that the response is antigen-specific because it requires the OVA-specific TCR present in the OT mice. For both OT-I and OT-II spleens, T cell activation could be detected when the adjuvant MPLA was included in the formulation, but no difference in activation status was observed between the cells that received free OVA + MPLA and the cells that received OVA co-administered with MPLA:N_3NLPs (Figure 2).

Enhanced OVA uptake but not activation of APCs with OVA:MPLA:NLPs in vitro

To determine the mechanism by which OVA:MPLA:N_3NLPs enhance OVA-specific T cell activation, we investigated the expression of activation markers by APC populations in the spleen, as our previous data indicated expression of these surface molecules can be enhanced by delivery of TLR agonists via NLPs *in vivo* [17]. WT splenocytes were cultured for 24 hours with the same treatments used to assess T cell activation, and while MPLA induced upregulation of activation markers by all APC subsets, no difference was observed between any of the MPLA-containing formulations, indicating that activation of APCs does not correlate with the T cell activation phenotype *in vitro* (Supplementary figure 1).

Next, we investigated the effect of OVA delivery via MPLA:N_3NLPs on the uptake of OVA by APCs. WT splenocytes were incubated with the same formulations above, prepared with OVA that had been fluorescently labeled with Alexa Fluor 488 (OVA-AF488), and uptake of OVA-AF488 was assessed by flow cytometry. In all cell types examined (DCs, macrophages, and B cells), significantly more cells were positive for OVA-AF488 upon treatment with OVA:MPLA:N_3NLPs than OVA, OVA+MPLA or OVA+MPLA:NLP (Figure 3). Internalization of

OVA-AF488 was confirmed by incubation with an AF488 quenching antibody, which quenches only the fluorescence of surface-bound OVA-AF488 while having no effect on internalized OVA-AF488 (Figure 3). Quenching of OVA-AF488 fluorescence was confirmed using permeabilized cells as a control (data not shown). These data suggest that attachment of OVA to MPLA:N_3NLPs enhances the uptake of OVA into APCs, thereby significantly enhancing antigen delivery to the same cells that receive MPLA.

Intranasal administration of OVA:MPLA:NLPs significantly increases T cell activation and expansion in lung-draining lymph nodes

To determine whether delivery of OVA on MPLA:N_3NLPs enhanced T cell responses *in vivo*, we transferred 10^6 OT-I or OT-II splenocytes to naïve WT mice and assessed the expansion (frequency of the OT-I/II TCR V$\beta5^+$ segment) and activation status of these cells in lymph nodes seven days following intranasal immunization. As expected, no OT-I/II expansion was detected in non-draining lymph nodes (Figure 4A and B). However, in the lung-draining lymph nodes, significant expansion of both OT-I and OT-II cells was observed 7 days post immunization. An increase in the percentage of cells expressing the OT-I/II TCR (Figure 4A and B), as well in the activation status of these V$\beta5^+$ cells (Figure 4C-E) was observed. Of particular note, unlike the *in vitro* activation experiments, an intermediate effect on OT-I cells was observed when OVA was co-administered with MPLA:N_3NLPs compared to OVA + free MPLA and OVA:MPLA:N_3NLPs (Figure 4D).

DISCUSSION

Due to the important and varied roles of T cells during infection, developing vaccine platforms that induce robust T cell responses is critically important. Here, we show that NLP-based delivery, previously shown to enhance antibody responses to protein antigens [18], also enhances the antigen-specific activation of T cells *in vitro* and *in vivo*.

The *in vitro* experiments suggest that the primary mechanism by which NLPs enhance T cell activation is through enhanced uptake of OVA, as evidenced by increased OVA-AF488 positive APCs when incubated with OVA-AF488:MPLA:N_3NLPs compared to OVA-AF488 + MPLA:N_3NLPs or OVA-AF488 + MPLA, while expression of costimulatory molecules on these same APCs was similar between all three groups. In contrast to the *in vitro* experiments, the *in vivo* activation of OT-I and OT-II cells suggests two mechanisms of action by which NLPs enhance T cell responses. Again, the fully conjugated OVA:MPLA:N_3NLP formulation induced significantly higher expansion and activation of T cells in draining lymph nodes. Notably, the OVA+MPLA:N_3NLP formulation had an intermediate effect between the OVA:MPLA:N_3NLP and OVA+MPLA formulations, with a clear trend in both the percent OT-I/II cells detected in the lymph nodes and in the activation status of these cells. These data suggest that in addition to enhanced delivery of OVA to APCs when incorporated onto NLPs, NLP-mediated delivery also enhanced the adjuvant effects of MPLA when MPLA:N_3NLPs were co-delivered with free OVA. These data are consistent with previous work from our laboratory, which showed increased uptake and activity of TLR agonists *in vivo* [17]. Other recent studies suggest nanoparticles can be used to expand subsets of $CD8^+$ and $CD4^+$ T cells with a regulatory-like phenotype [30-32], promoting the induction of tolerance against self-peptides rather than a classic T cell

response that is desired against pathogen-derived peptides. In those studies, mice received repeated doses of unadjuvanted nanoparticles, in contrast to our current study where mice received a single dose of NLPs formulated with antigen and MPLA adjuvant. Ultimately, studies aimed at determining the mechanism by which nanoparticles enhance both types of responses will aid the fine-tuning of formulations and dosing regimens for elicitation of a specific desired response.

Importantly, the enhanced activation of T cells was observed for both $CD4^+$ and $CD8^+$ cells, indicating that NLP-mediated delivery achieves both standard exogenous antigen presentation on MHC-II and cross-presentation on MHC-I. Several factors have been shown to have positive effects on antigen cross-presentation to $CD8^+$ T cells *in vitro* and *in vivo* including various innate immune stimuli, increasing effective antigen doses by antigen clustering (e.g. use of particles) and targeting of antigen to APCs [33-37]. Interestingly, the two mechanisms of action of NLPs predicted by our results contribute to enhancing cross-presentation: 1) NLPs enhance the adjuvant effects of TLR agonists on innate immune cells, leading to a more activated/mature phenotype [17]; and 2) the enhanced uptake of OVA leads to a higher *effective* dose of antigen delivered to these same APCs. The relative contribution of increased OVA uptake by APCs and potential trafficking/targeting of OVA-containing NLPs to APCs *in vivo* has not yet been determined. Ultimately, this ability of NLPs to simultaneously enhance adjuvant and antigen effective doses to allow cross-presentation will be important for the application of the NLP platform to vaccines in which cell-mediated immunity is desired.

Current data suggest that both the magnitude and quality of T cell responses to a vaccine candidate is important to achieve the desired protective outcomes [1]. Our work

demonstrates that NLPs significantly enhance the magnitude of T cell responses to a protein antigen upon immunization. While this was shown for both $CD4^+$ and $CD8^+$ T lymphocytes, further work is needed to determine the specific types of responses induced and to determine to what extent the observed effects are dependent on the specific antigen. The potential for incorporating other TLR agonists and antigens into NLPs will allow these questions to be addressed and has important implications for vaccine design, potentially allowing "tuning" of the immune response for each target pathogen according to known protective mechanisms.

REFERENCES

[1] Gilbert SC. T-cell-inducing vaccines – what's the future. Immunology. 2012;135:19-26.
[2] Sahdev P, Ochyl L, Moon J. Biomaterials for nanoparticle vaccine delivery systems. Pharmaceutical Research. 2014:1-20.
[3] Reed SG, Bertholet S, Coler RN, Friede M. New horizons in adjuvants for vaccine development. Trends in Immunology. 2009;30:23-32.
[4] Aguilar JC, Rodríguez EG. Vaccine adjuvants revisited. Vaccine. 2007;25:3752-62.
[5] Leleux J, Roy K. Micro and nanoparticle-based delivery systems for vaccine immunotherapy: An immunological and materials perspective. Advanced Healthcare Materials. 2013;2:72-94.
[6] Zhao L, Seth A, Wibowo N, Zhao C-X, Mitter N, Yu C, et al. Nanoparticle vaccines. Vaccine. 2014;32:327-37.
[7] Krishnamachari Y, Geary S, Lemke C, Salem A. Nanoparticle delivery systems in cancer vaccines. Pharm Res. 2011;28:215-36.
[8] Look M, Bandyopadhyay A, Blum JS, Fahmy TM. Application of nanotechnologies for improved immune response against infectious diseases in the developing world. Advanced Drug Delivery Reviews. 2010;62:378-93.
[9] Shen H, Ackerman AL, Cody V, Giodini A, Hinson ER, Cresswell P, et al. Enhanced and prolonged cross-presentation following endosomal escape of exogenous antigens encapsulated in biodegradable nanoparticles. Immunology. 2006;117:78-88.
[10] Kuchtey J, Chefalo PJ, Gray RC, Ramachandra L, Harding CV. Enhancement of dendritic cell antigen cross-presentation by cpg DNA involves type i ifn and stabilization of class i mhc mrna. The Journal of Immunology. 2005;175:2244-51.
[11] Ulevitch RJ. Therapeutics targeting the innate immune system. Nat Rev Immunol. 2004;4:512-20.
[12] Persing DH, Coler RN, Lacy MJ, Johnson DA, Baldridge JR, Hershberg RM, et al. Taking toll: Lipid a mimetics as adjuvants and immunomodulators. Trends in Microbiology. 2002;10:s32-s7.

[13] Baldridge JR, McGowan P, Evans JT, Cluff C, Mossman S, Johnson D, et al. Taking a toll on human disease: Toll-like receptor 4 agonists as vaccine adjuvants and monotherapeutic agents. Expert Opin Biol Ther. 2004;4:1129-38.
[14] Baldridge JR, Yorgensen Y, Ward JR, Ulrich JT. Monophosphoryl lipid a enhances mucosal and systemic immunity to vaccine antigens following intranasal administration. Vaccine. 2000;18:2416-25.
[15] Steinhagen F, Kinjo T, Bode C, Klinman DM. Tlr-based immune adjuvants. Vaccine. 2011;29:3341-55.
[16] Fischer NO, Weilhammer DR, Dunkle A, Thomas C, Hwang M, Corzett M, et al. Evaluation of nanolipoprotein particles (nlps) as an in vivo delivery platform. PLoS One. 2014;9:e93342.
[17] Weilhammer DR, Blanchette CD, Fischer NO, Alam S, Loots GG, Corzett M, et al. The use of nanolipoprotein particles to enhance the immunostimulatory properties of innate immune agonists against lethal influenza challenge. Biomaterials. 2013;34:10305-18.
[18] Fischer NO, Rasley A, Corzett M, Hwang MH, Hoeprich PD, Blanchette CD. Colocalized delivery of adjuvant and antigen using nanolipoprotein particles enhances the immune response to recombinant antigens. J Am Chem Soc. 2013;135:2044-7.
[19] Shen L, Higuchi T, Tubbe I, Voltz N, Krummen M, Pektor S, et al. A trifunctional dextran-based nanovaccine targets and activates murine dendritic cells, and induces potent cellular and humoral immune responses <italic>in vivo</italic>. PLoS ONE. 2013;8:e80904.
[20] Wilson JT, Keller S, Manganiello MJ, Cheng C, Lee C-C, Opara C, et al. Ph-responsive nanoparticle vaccines for dual-delivery of antigens and immunostimulatory oligonucleotides. ACS Nano. 2013;7:3912-25.
[21] Stano A, Nembrini C, Swartz MA, Hubbell JA, Simeoni E. Nanoparticle size influences the magnitude and quality of mucosal immune responses after intranasal immunization. Vaccine. 2012;30:7541-6.
[22] Teijaro JR, Turner D, Pham Q, Wherry EJ, Lefrançois L, Farber DL. Cutting edge: Tissue-retentive lung memory cd4 t cells mediate optimal protection to respiratory virus infection. The Journal of Immunology. 2011;187:5510-4.
[23] Turner DL, Bickham KL, Thome JJ, Kim CY, D'Ovidio F, Wherry EJ, et al. Lung niches for the generation and maintenance of tissue-resident memory t cells. Mucosal Immunol. 2014;7:501-10.
[24] Farber DL, Yudanin NA, Restifo NP. Human memory t cells: Generation, compartmentalization and homeostasis. Nat Rev Immunol. 2014;14:24-35.
[25] Cauley LS, Lefrancois L. Guarding the perimeter: Protection of the mucosa by tissue-resident memory t cells. Mucosal Immunol. 2013;6:14-23.
[26] Blanchette C, Segelke B, Fischer N, Corzett M, Kuhn E, Cappuccio J, et al. Characterization and purification of polydisperse reconstituted lipoproteins and nanolipoprotein particles. International Journal of Molecular Sciences. 2009;10:2958-71.
[27] Blanchette CD, Law R, Benner WH, Pesavento JB, Cappuccio JA, Walsworth V, et al. Quantifying size distributions of nanolipoprotein particles with single-particle analysis and molecular dynamic simulations. Journal of Lipid Research. 2008;49:1420-30.
[28] Blanchette CD, Fischer NO, Corzett M, Bench G, Hoeprich PD. Kinetic analysis of his-tagged protein binding to nickel-chelating nanolipoprotein particles. Bioconjugate Chemistry. 2010;21:1321-30.

[29] Fischer NO, Blanchette CD, Chromy BA, Kuhn EA, Segelke BW, Corzett M, et al. Immobilization of his-tagged proteins on nickel-chelating nanolipoprotein particles. Bioconjugate Chemistry. 2009;20:460-5.
[30] Tsai, S., A. Shameli, J. Yamanouchi, X. Clemente-Casares, J. Wang, P. Serra, Y. Yang, Z. Medarova, A. Moore and P. Santamaria (2010). "Reversal of Autoimmunity by Boosting Memory-like Autoregulatory T Cells." Immunity **32**(4): 568-580.
[31] Clemente-Casares, X., J. Blanco, P. Ambalavanan, J. Yamanouchi, S. Singha, C. Fandos, S. Tsai, J. Wang, N. Garabatos, C. Izquierdo, S. Agrawal, M. B. Keough, V. W. Yong, E. James, A. Moore, Y. Yang, T. Stratmann, P. Serra and P. Santamaria (2016). "Expanding antigen-specific regulatory networks to treat autoimmunity." Nature **530**(7591): 434-440.
[32] Bayry, J. (2016). "Repressing Immunity in Autoimmune Disease." New England Journal of Medicine **374**(21): 2090-2092.
[33] Wagner CS, Cresswell P. Tlr and nucleotide-binding oligomerization domain-like receptor signals differentially regulate exogenous antigen presentation. The Journal of Immunology. 2012;188:686-93.
[34] Brossart P, Bevan MJ. Presentation of exogenous protein antigens on major histocompatability complex class i molecules by dendritic cells: Pathway of presentation and regulation by cytokines. Blood. 1997;90:1594-9.
[35] Bowers EV, Horvath JJ, Bond JE, Cianciolo GJ, Pizzo SV. Antigen delivery by α 2-macroglobulin enhances the cytotoxic t lymphocyte response. Journal of Leukocyte Biology. 2009;86:1259-68.
[36] Howland SW, Tsuji T, Gnjatic S, Ritter G, Old LJ, Wittrup KD. Inducing efficient cross-priming using antigen-coated yeast particles. Journal of immunotherapy (Hagerstown, Md : 1997). 2008;31:607.
[37] Wang B, Kuroiwa JMY, He L-Z, Charalambous A, Keler T, Steinman RM. The human cancer antigen mesothelin is more efficiently presented to the mouse immune system when targeted to the dec-205/cd205 receptor on dendritic cells. Annals of the New York Academy of Sciences. 2009;1174:6-17.

Figure 1: Generation of OVA:MPLA:N_3NLPs

A. Diagram of basic MPLA:N_3NLP assembly reaction & attachment of OVA by click chemistry. Scaffold protein (human apoE422k), lipid (1,2-dioleoyl-sn-glycero-3-phosphocholine (DOPC), C18-PEG6-N_3, monophosphoryl lipid A (MPLA), and surfactant (cholate) are combined, and MPLA:N_3NLPs self-assemble upon dialysis of the surfactant. OVA is linked to DBCO (OVA-DBCO), an alkyne-containing compound, which reacts with N_3 to covalently attach OVA-DBCO to assembled MPLA:N_3NLPs. **B.** Detection of attachment of OVA-DBCO to MPLA:N_3NLPs using size-exclusion chromatography (SEC). Two peaks are clearly visible in the SEC traces of preparations using different OVA-DBCO to MPLA:N_3NLP ratios as noted. The first peak corresponds to the MPLA:N_3NLP and the second peak corresponds to unreacted OVA-DBCO. **C.** To quantify conjugation efficiency, NLPs reacted with OVA were purified by SEC, dissociated in SDS, and analyzed by SDS-PAGE (inset). By comparing band intensity to appropriate protein standards, the actual molar ratio of OVA-DBCO attached to the MPLA:N_3NLP (OVA:MPLA:N_3NLP actual) as a function of the initial reaction ratio (OVA:MPLA:N_3NLP input) was determined.

Figure 2: Activation of OT-I and OT-II T cells by OVA:MPLA:NLPs *in vitro*

Splenocytes from wild type (WT), OT-I, and OT-II mice were incubated with 3 μg/ml OVA +/- 0.41 μg/ml MPLA in different formulations (PBS and OVA alone included as controls) for 24 h, and T cells were analyzed for expression of activation markers by flow cytometry. Representative histograms of CD25, CD69, and CD44 expression (pregated on $CD3^+$ cells) from OT-I cells are shown (**A**). The mean + S.D. from triplicate wells from a single

experiment (out of 2 (OT-II) or 3 (OT-I)) are shown in **B**. Data were analyzed by 2-way ANOVA, and p values for multiple comparisons within each cell type are shown (*p < 0.05, **p < 0.01, ***p < 0.001, **** p < 0.0001).

Figure 3: Uptake of OVA into APCs

Splenocytes from WT C57BL/6 mice were incubated with 3 μg/ml Alexa Fluor 488-labeled OVA (OVA-AF488) +/- 0.25 μg/ml MPLA in different formulations (PBS and OVA-AF488 alone included as controls) for 1 h. Cells were surface stained for APC markers, then incubated with an AF488 quenching antibody, before analysis by flow cytometry. Data is shown as the mean percentage of OVA-AF488 positive cells + S.D. of duplicate wells from a representative experiment (out of 2). Data were analyzed by one-way ANOVA with multiple comparisons (*p < 0.05, **p < 0.01).

Figure 4: Activation of OVA-specific T cells *in vivo* in lung-draining lymph nodes following intranasal immunization

WT C57BL/6 mice were seeded with 10^6 splenocytes from OT-I (**A**) or OT-II (**B**) mice by intraperitoneal injection one day before immunization. Mice were immunized intranasally with OVA + MPLA in different formulations: PBS control; OVA alone; OVA + MPLA (free); OVA + MPLA:NLPs (coadministration); and OVA:MPLA:NLPs (fully conjugated particle-based co-delivery). Expansion of OT-I/II cells was examined on day 7 in lung-draining and non-draining (inguinal) lymph nodes (LNs) by detection of TCR $V\beta5^+$ cells within $CD8^+$ (A) or $CD4^+$ (B) populations. Baseline percentages of $V\beta5^+$ cells are reflected in PBS and non-draining LN samples. **C, D, E**. Activation status of $V\beta5^+$ cells. $V\beta5^+$ cells from the

experiments in A and B were stained for expression of CD62L and CD44 to distinguish naïve cells from effector/memory cells. Plots representing Vβ5$^+$ (OT-I) cells from non-draining LNs (NDLN) or lung-draining LNs (LDLN) immunized with PBS (showing baseline levels) or OVA:MPLA:NLPs (showing maximal activation) are shown in (**C**). Data for all groups from three (OT-I, **D**) or one (OT-II, **E**) experiments are shown on the left. Data in A, B, D, and E were analyzed by one-way ANOVA with multiple comparisons (*$p < 0.05$, **$p < 0.01$, ***$p < 0.001$, **** $p < 0.0001$)

481 Figure 1

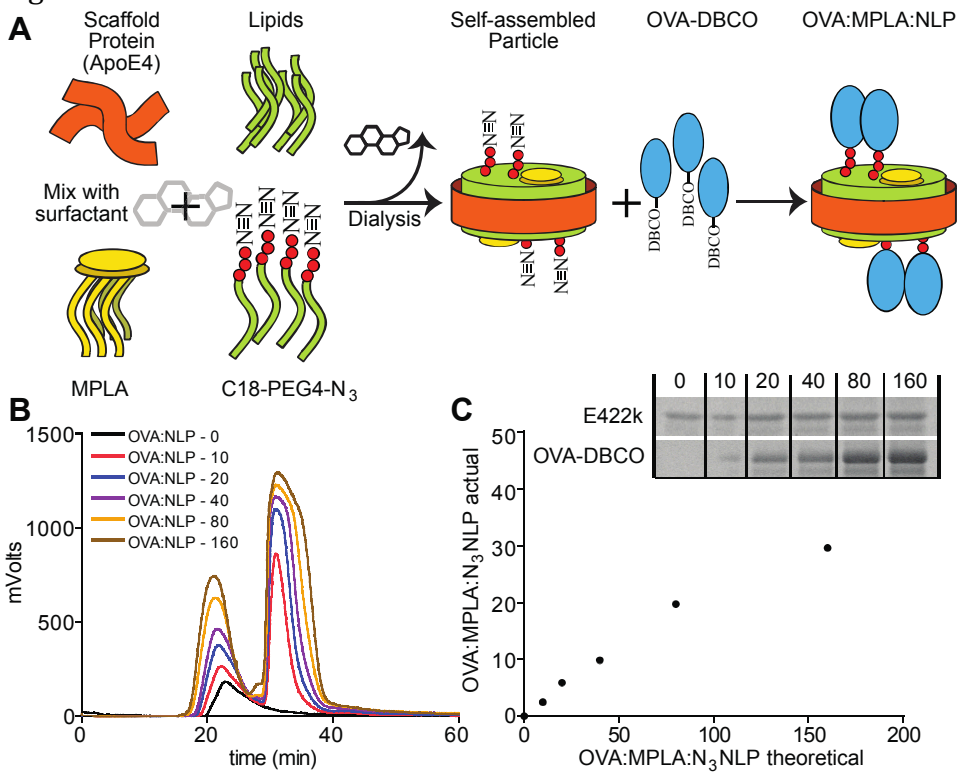

482
483
484

Figure 2

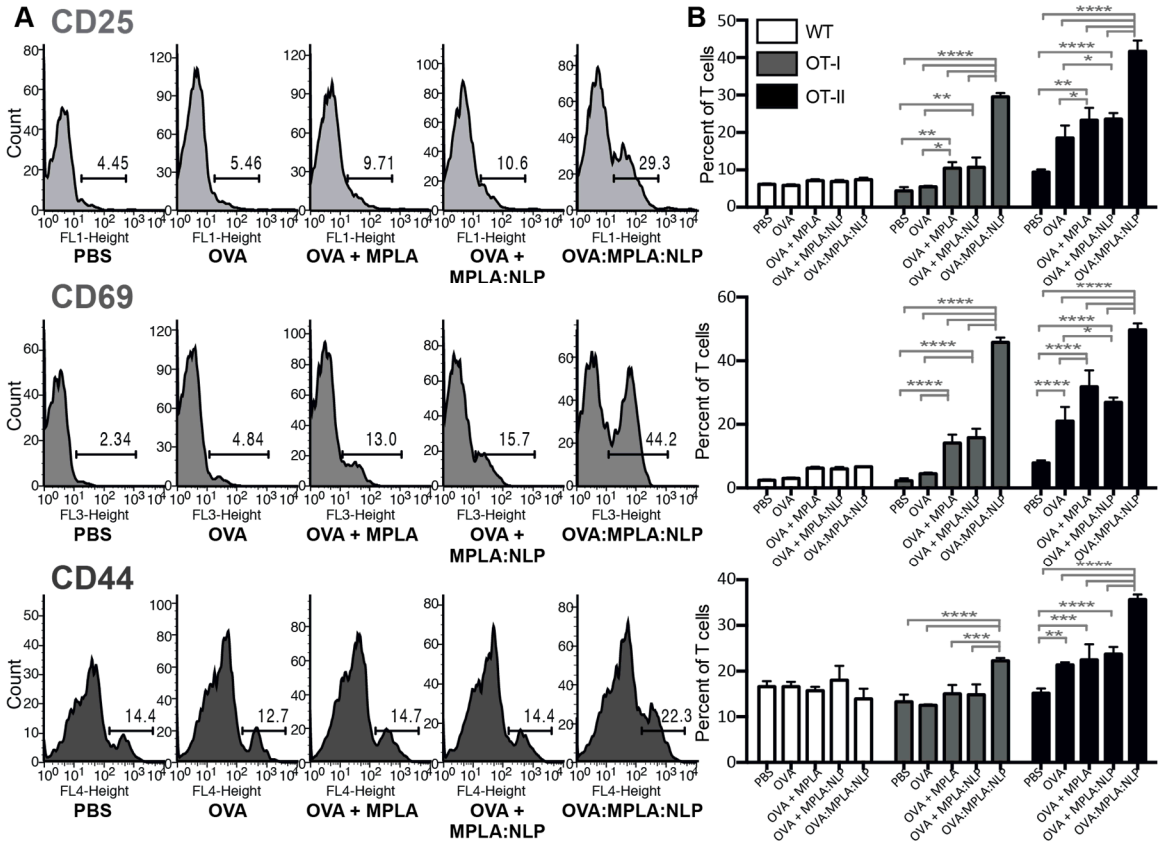
A
CD25
CD69
CD44
Count
FL1-Height
FL3-Height
FL4-Height
4.45
5.46
9.71
10.6
29.3
2.34
4.84
13.0
15.7
44.2
14.4
12.7
14.7
14.4
22.3
PBS
OVA
OVA + MPLA
OVA + MPLA:NLP
OVA:MPLA:NLP
B
WT
OT-I
OT-II
Percent of T cells

Figure 3

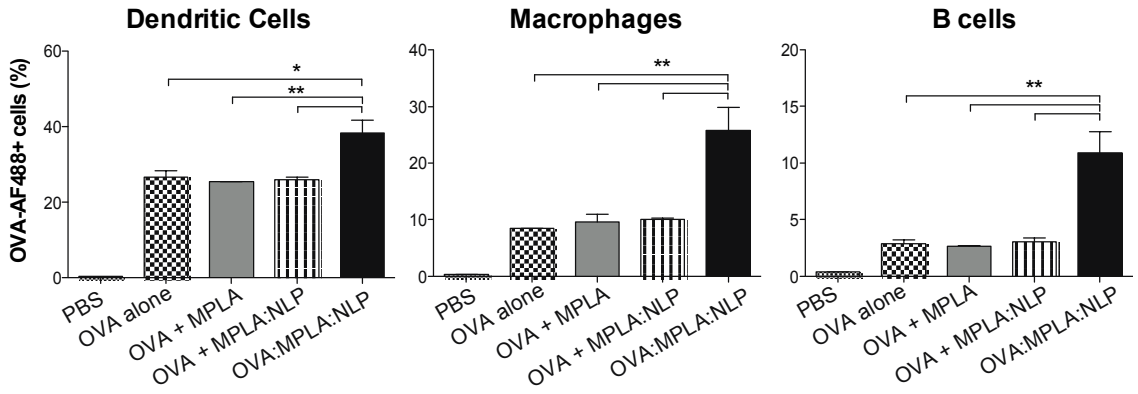

Figure 4